# Developmental Regulation of Indole-3-Acetic Acid Turnover in Scots Pine Seedlings[1]

**Karin Ljung[2], Anders Östin[2,3], Laetitia Lioussanne, and Göran Sandberg***

Department of Forest Genetics and Plant Physiology, The Swedish University of Agricultural Sciences, S–901 83 Umeå, Sweden

Indole-3-acetic acid (IAA) homeostasis was investigated during seed germination and early seedling growth in Scots pine (*Pinus sylvestris*). IAA-ester conjugates were initially hydrolyzed in the seed to yield a peak of free IAA prior to initiation of root elongation. Developmental regulation of IAA synthesis was observed, with tryptophan-dependent synthesis being initiated around 4 d and tryptophan-independent synthesis occurring around 7 d after imbibition. Induction of catabolism to yield 2-oxindole-3-acetic acid and irreversible conjugation to indole-3-acetyl-*N*-aspartic acid was noticed at the same time as de novo synthesis was first detected. As a part of the homeostatic regulation IAA was further metabolized to two new conjugates: glucopyranosyl-1-*N*-indole-3-acetyl-*N*-aspartic acid and glucopyranosyl-1-*N*-indole-3-acetic acid. The initial supply of IAA thus originates from stored pools of IAA-ester conjugates, mainly localized in the embryo itself rather than in the general nutrient storage tissue, the megagametophyte. We have found that de novo synthesis is first induced when the stored pool of conjugated IAA is used up and additional hormone is needed for elongation growth. It is interesting that when de novo synthesis is induced, a distinct induction of catabolic events occurs, indicating that the seedling needs mechanisms to balance synthesis rates for the homeostatic regulation of the IAA pool.

Indole-3-acetic acid (IAA) is a well-known regulator of plant growth and development, which is active in submicromolar amounts and is associated with a variety of physiological processes, including apical dominance, tropisms, shoot elongation, induction of cambial cell division, and lateral root initiation. The IAA content of plant tissues is believed to be regulated by several processes. De novo synthesis and the hydrolysis of IAA conjugates represent inputs into the IAA pool, which can be counterbalanced by a variety of conjugative and catabolic pathways (Normanly, 1997; Normanly and Bartel, 1999). IAA levels in individual tissues can also be influenced by the basipetal polar transport system, which results in the downward movement of IAA from apical tissue and young leaves toward the root system (Estelle, 1998). However, the exact mechanism whereby auxin controls growth and development is not clear. It has been proposed that the concentration of the hormone, the ratio of IAA to other plant hormones, and the sensitivity of tissues to IAA may all be primary determinants of auxin action (Normanly, 1997). The balance between IAA biosynthesis, metabolism, and transport, or IAA homeostasis is a dynamic process that responds to developmental and environmental signals (Miller et al., 1987; Michalczuk et al., 1992; Bandurski et al., 1995; Tam et al., 1995). This homeostatic balance is, therefore, a potential key element in the regulation of auxin action. A major problem in clarifying the possible relationships in the homeostatic regulation of IAA is the lack of knowledge about factors contributing to these mechanisms such as biosynthesis, metabolism, transport, and signal perception and transduction.

The biosynthesis of IAA in plants is still not fully understood and there are reasons to believe that several pathways exist (Bartel, 1997). Today most attention is focused on the relationship between the Trp-dependent and a possible Trp-independent pathway of IAA synthesis (Normanly et al., 1993, 1995). We have recently presented evidence suggesting that these two pathways are operational in tobacco during vegetative growth (Sitbon et al., 2000). Utilization of dual pathways has also been described in carrot cell cultures where different IAA biosynthesis pathways operate in callus cultures compared with developing somatic embryos (Michalczuk et al., 1992; Ribnicky et al., 1996). In the study presented here we have analyzed possible developmental regulation of the two putative pathways.

The first comprehensive attempt to measure the different components comprising the IAA homeostasis mechanism, published in 1980 by Epstein et al., elegantly showed that the maize kernel utilizes stored forms of IAA for initial seedling growth. We have chosen germinating Scots pine (*Pinus sylvestris*) seedlings for our experiments since this is one of the few species for which we have an extensive overview of the catabolic and conjugative pathways (Andersson and Sandberg, 1982; Sandberg, 1984; Ernstsen

[1] This work was supported by The Swedish Council of Forestry and Agricultural Research and The Foundation for Strategic Research.

[2] These authors contributed equally to the paper.

[3] Present address: National Institute of Working Life, S–907 13 Umeå, Sweden.

* Corresponding author; e-mail goran.sandberg@genfys.slu.se; fax 46–90–7865901.

and Sandberg, 1986; Ernstsen et al., 1987, Sandberg et al., 1987). A further advantage of this system is that the initial growth of the seedling is almost exclusively due to cell elongation, and only to a minor extent to cell division (Sandberg et al., 1987).

In this study we have considered the major components supplying the IAA pool, as well as the metabolic components involved in its regulation. We have investigated the developmental control of these mechanisms and have shown that the induction of key elements of IAA metabolism is strongly correlated with major physiological and morphological events. We have also identified two new IAA conjugates in germinating Scots pine seedlings, two *N*-linked hexoses of IAA and indole-3-acetyl aspartic acid (IAAsp), probably glucosides. This type of conjugation to an intact indole nucleus has not previously been described in plants.

## RESULTS

### Seed Development during Germination

When Scots pine seeds are germinating (Fig. 1A), the first visible change occurs 2 d after imbibition when the secondary wall in the cortex of the embryo hypocotyl starts to develop. During the 3rd d, the secondary wall continues to develop, and swelling caused by a general cell enlargement starts to separate the two halves of the seed coat. At the same time the first increment in cell length in the hypocotyl occurs, which leads to the root cap penetrating the nucellus and reaching the opening in the seed coat. Between d 3 and 4, the hypocotyl and root elongate rapidly, with the hypocotyl ending its elongation growth around d 8. The main root continues to grow at approximately the same rate for the rest of the period covered in our experiments. The elongation of the cotyledons is somewhat delayed, being induced at around d 5 and continuing for the remainder of the 12 d analyzed, although at a slower rate after d 10. Figure 1B shows the germination percentage of the Scots pine seeds.

### Quantification of IAA and IAA Conjugates

Free IAA and conjugated IAA were analyzed over a period of 10 d following imbibition (Fig. 1C), and with the use of different strengths of hydrolysis, it was possible to distinguish between the pools of amide-linked and ester-linked conjugates. A rapid increase in the content of free IAA was observed in the first few days following imbibition, reaching a maximum of 100 ng/g of tissue after 48 h. This dramatic increase in free IAA was correlated with a decrease in the pool of ester-linked conjugates during the first 60 h. It is interesting that the high level of

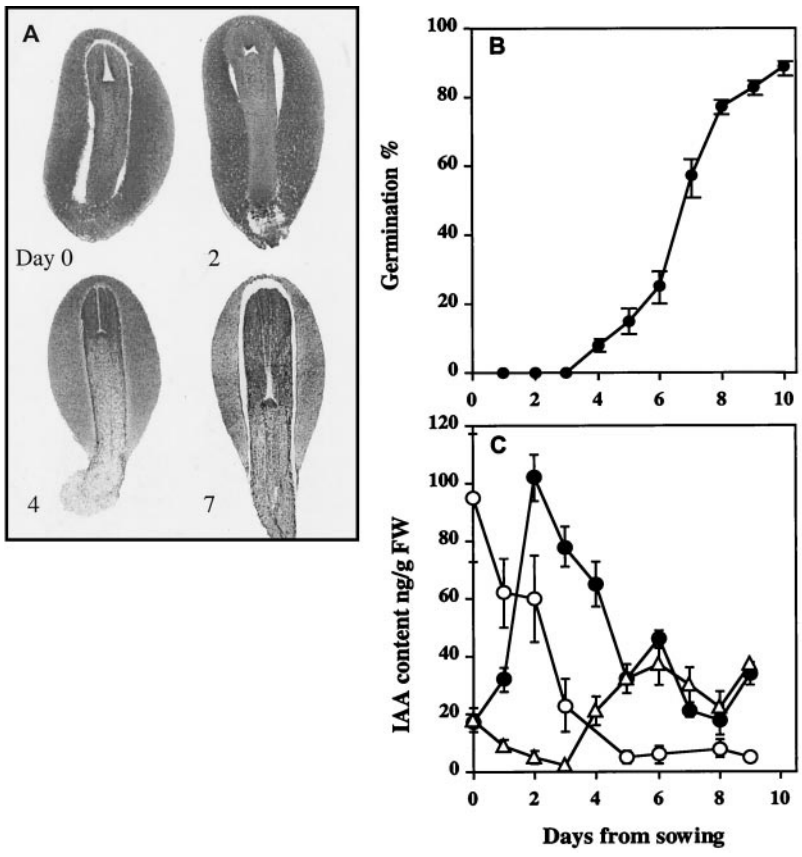


**Figure 1.** A, Sections of germinating seeds 0, 2, 4, and 7 d after imbibition. B, Percentage germination of Scots pine seeds. C, Levels of free IAA (●) and ester-linked (○) and amide-linked (△) conjugates of IAA in Scots pine seeds 0 to 10 d after imbibition. Vertical bars represent SD. FW, Fresh weight.

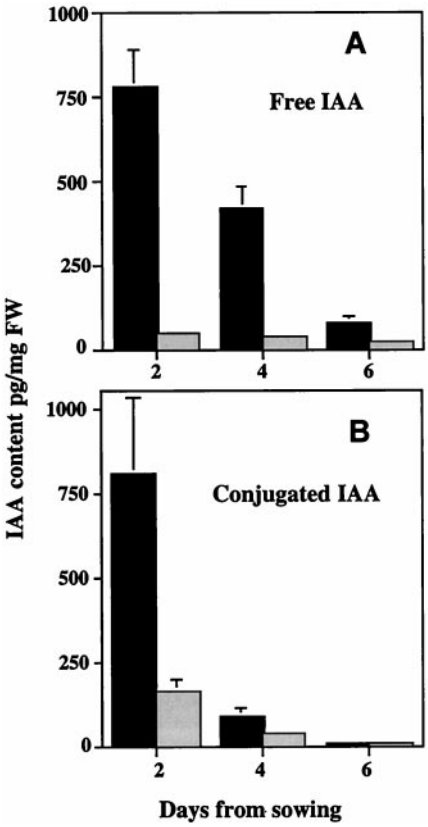


**Figure 2.** Levels of free (A) and conjugated IAA (B) in the megagametophyte (gray bars) and embryo (black bars) of Scots pine seeds 2, 4, and 6 d after imbibition. Vertical bars represent SD. FW, Fresh weight.

free IAA observed after 48 h decreased when root elongation was initiated. Amide conjugates were not a significant component of the stored IAA in the dry seed. However, this category of IAA conjugates increased when root elongation was initiated. The pulse of free IAA observed is in agreement with IAA profiles previously obtained from Scots pine (Sandberg et al., 1987) and spruce (Sandberg and Ernstsen, 1987) using HPLC fluorescence detection analysis. To determine where the stored IAA was localized, embryos were dissected out from seeds 2, 4, and 6 d after imbibition. The content of free and conjugated IAA (amide- + ester-linked) was then determined in the embryo and in the megagametophyte. We also attempted this dissection at the start of imbibition, but without success since the megagametophyte was too compact to allow separation of the fragile embryo. Data shown in Figure 2 demonstrate that the majority of free (Fig. 2A) and conjugated (Fig. 2B) IAA is localized in the embryo and not the megagametophyte. Furthermore, the trend of IAA declining with time observed for the entire seed (Fig. 1C) was also observed in the embryo. The conjugated IAA was almost completely consumed within 6 d of imbibition.

### IAA Biosynthesis from [$^{15}N_1$]Trp and Deuterated Water

A study was performed to investigate the stage of development at which IAA biosynthesis is initiated during germination and initial seedling growth. First, to give the tissue a pulse of tracer, seeds and seedlings were incubated with [$^{15}N_1$]Trp for 6 h and the appearance of [$^{15}N_1$]IAA was measured during the following 48 h. A relatively low amount of the added Trp (about 20% of the total) was taken up. Thus the increase in the seeds Trp pool caused by adding label was small (data not shown). Figure 3A shows the relative abundance of synthesized [$^{15}N_1$]IAA. Linked gas chromatography mass spectrometry (GC-MS) analysis of IAA from the incubation starting on d 1 and ending on d 3 showed no significant increase in *m/z* 203, whereas the experiment that started on d 4 and ending on d 6 showed a significant increase in *m/z* 203. It can thus be concluded that there is no de novo synthesis of IAA from Trp before d 3, and that this pathway is induced between d 4 and 6. However, there appears to be no further increase in synthesis

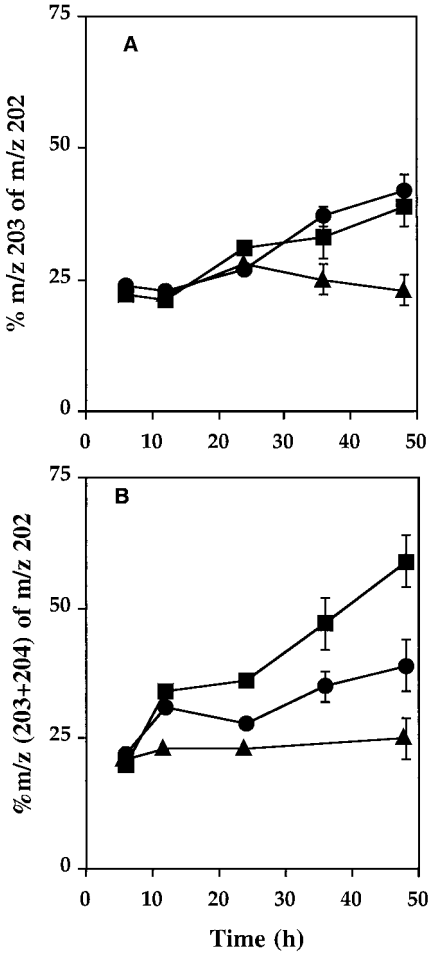


**Figure 3.** IAA synthesis from [$^{15}N_1$]Trp (A) and $^2H_2O$ (B). Relative incorporation of $^{15}N_1$ and $^2H$ are expressed as the ratios of *m/z* 203/202 and (203 + 204)/202, respectively. Incubation initiated at d 1 (▲), d 4 (●), and d 7 (■). Vertical bars represent SD.

**Table I.** *Turnover of IAA in germinating seeds of Scots pine*

Information on the [$^{12}C_6$]IAA content, [$^{13}C_6/^{12}C_6$]IAA ratio, and [$^{13}C_6$]IAA half-life. Values are means of four to six replicates; SD as indicated.

| Parameter | Day of Germination | | |
|---|---|---|---|
| | 1 | 4 | 7 |
| [$^{12}C_6$]IAA content ng/g ($t = 0$) | 35 ± 4 | 72 ± 6 | 31 ± 6 |
| Ratio [$^{13}C_6/^{12}C_6$]IAA ($t = 0$) | 0.13 ± 0.06 | 0.39 ± 0.12 | 0.24 ± 0.09 |
| Half life of [$^{13}C_6$]IAA (hours) | >48 | 16.4 ± 4.1 | 7.2 ± 2.3 |

from this pathway after d 6, according to results from the incubation starting at d 7 and ending at d 9.

Not all synthesis of IAA is believed to involve Trp as a precursor (Normanly et al., 1993; Bartel, 1997). To investigate whether any IAA synthesis pathways other than the Trp-mediated pathway are induced during germination, seeds and seedlings were incubated with deuterated water for 48-h periods starting at d 1, 4, and 7. Figure 3B shows the relative abundance of synthesized [$^2$H]IAA. In accordance with the study of Trp-dependent synthesis described above, no incorporation of $^2$H into IAA was observed when the seeds were incubated for 48 h starting at d 1. Also in accordance with the $^{15}$N experiment, clear evidence of induction was observed (i.e. incorporation of $^2$H into IAA) between d 4 and 6. However, a further increase in incorporation rate was obtained when the incubation was started at d 7. It can thus be concluded that an additional IAA synthesis pathway is induced after d 6 and that this synthesis is not mediated via Trp.

### Turnover of [$^{13}C_6$]IAA

Turnover of [$^{13}C_6$]IAA was analyzed 1, 4, and 7 d after imbibition. The [$^{13}C_6/^{12}C_6$]IAA ratio at the start of the experiments ranged from 0.13 to 0.39 (Table I). The disappearance of label from the IAA pool followed first order kinetics, which simplified the calculation of IAA half-life. There was almost no turnover of IAA during the first 3 d of imbibition since the half-life was more than 48 h when the experiment started 1 d after imbibition. After 4 d, however, turnover had clearly been initiated, giving a half-life at this point of 16.4 h. This was even more pronounced after 7 d, when the half-life was 7.2 h. Another noteworthy result was the difference between experiments in [$^{13}C_6/^{12}C_6$]IAA ratio observed after the initial 5-h incubation period. Clear indications of an induction of IAA uptake was detected between d 1 and 4. This difference is even more pronounced if the increase in the endogenous IAA pool that occurs between d 1 and 4 is taken into account.

### Identification of IAA Metabolites

Incubation of seedlings with $^{14}$C-labeled IAA led to the formation of six metabolites that were designated metabolites 1 through 6 in order of decreasing polarity (Fig. 4). Metabolites 1 and 2 had retention times of 0.06 and 0.25 relative to IAA that changed, after methylation, to 0.77 for both substances. No conclusive identity of these very polar catabolites was obtained by HPLC-MS analysis.

The methylated and acetylated derivative of metabolite 3 had molecular ions $[M + H]^+$ of *m/z* 649/655 (Fig. 5A), corresponding to the incorporation of four acetyl groups into the Glc moiety. This was further supported by diagnostic ions of the acetylated Glc observed at *m/z* 43, 109, 169, 229, and 331. The molecular ions $[M + H]^+$ *m/z* 649/655 were analyzed by constant magnetic sector/electric sector (B/E)-linked scanning (Fig. 5A). Both spectra described the loss of a methyl ester [$M-CH_3O$] (*m/z* 617/623), loss of an acetyl group [$M-COCH_3$] (*m/z* 607/613), and loss of acetic acid (from an acetylated hydroxy group) [$M-OCOCH_3$] (*m/z* 590/596). The indole moiety was described by the quinolinium ion (*m/z* 130/136), the quinolinium ion with a retained acetylated sugar moiety at *m/z* 460/466, and the loss of methylated Asp, giving an *m/z* 487/493 ion. The acetylated hexose moiety gave a series of diagnostic ions with *m/z* 109, 169, 211, 271, and 331. The relative intensity of these ions was compared with the daughter ions obtained from acetylated hexose standards using *m/z* 331 as parent ion. An intense *m/z* 169 ion was produced, excluding the possibility that Fru is the hexose moiety, since it usually gives an intense *m/z* 211. Furthermore, the fact that *m/z* 211 has a lower intensity than *m/z* 271 indicates that the sugar is Glc. Mass determination of the $[M + H]^+/[^{13}C_6M + H]^+$ of metabolite 3 at a resolution of 5,000 gave *m/z* 649.228/655.243 and a calculated elemental composi-

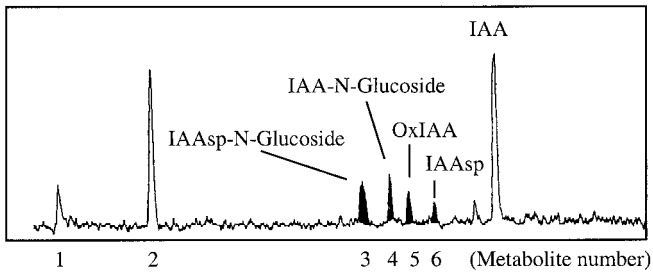


**Figure 4.** Metabolic HPLC-RC profile from Scots pine seedlings showing the major IAA metabolites. Ten-day-old seedlings were incubated for 24 h with media containing [$^{14}$C]IAA. After extraction and purification the IAA metabolites were separated by HPLC-RC.

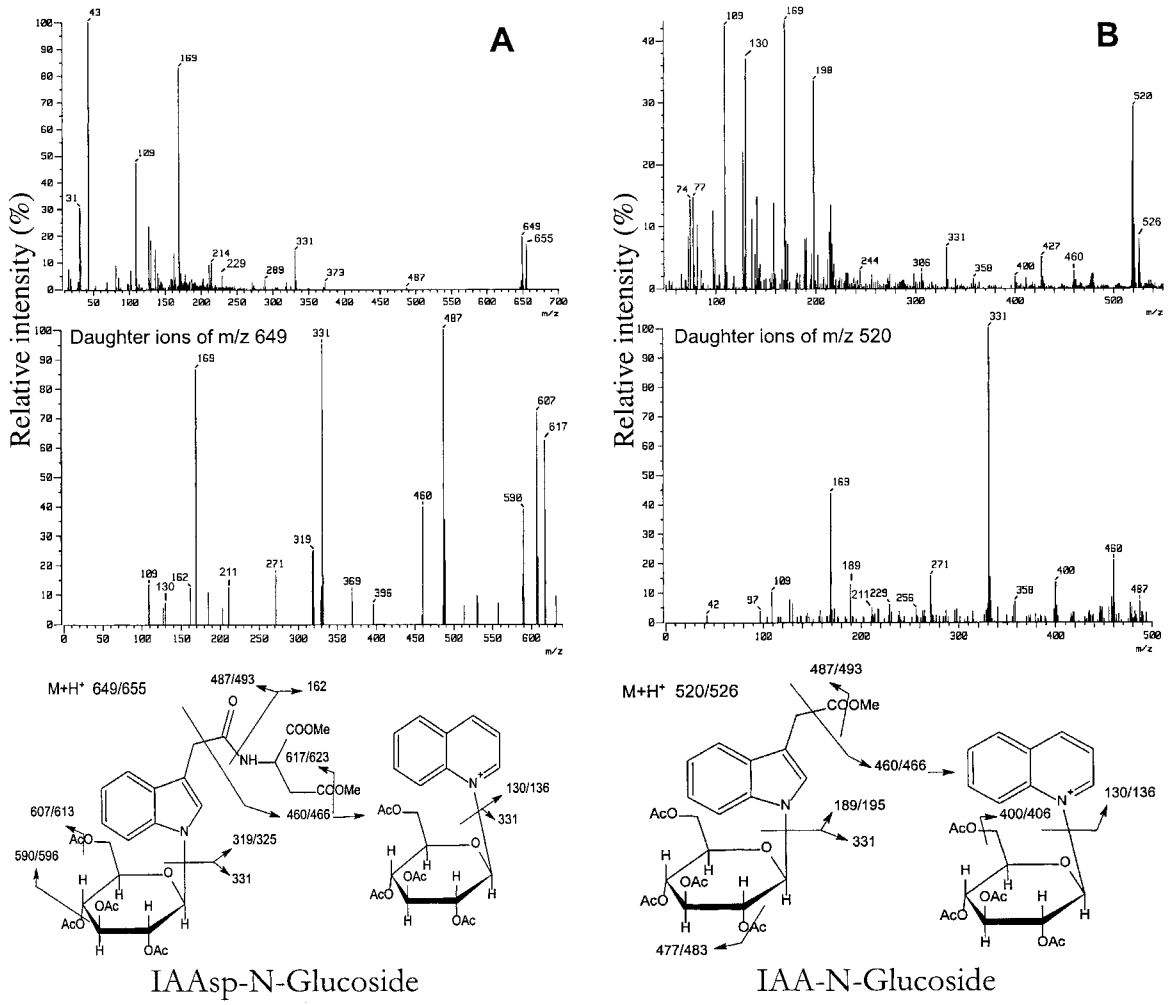


**Figure 5.** HPLC-frit-FAB mass spectra (top), B/E-linked scan daughter ion spectra (middle), and proposed fragmentation pattern (bottom) of methylated and acetylated IAAsp-*N*-glucoside (A) and IAA-*N*-glucoside (B) isolated from Scots pine shoots.

tion of $C_{30}H_{37}O_{14}N_2/^{12}C_{24}{}^{13}C_6H_{37}O_{14}N_2$ (theoretical value = *m/z* 649.2242/655.2444). The protonated molecular ion of the methylated form of metabolite 3, *m/z* 481/487 (non-labeled/[$^{13}C_6$]-labeled), and the extracted ion chromatograms also indicated that this metabolite was a glucosylated IAA conjugate (Fig. 6A). Verified daughter ions from *m/z* 481/487 were *m/z* 130/136, 162/162, 319/325, and 361/367. These ions describe the loss of a quinolinium ion of *m/z* 130/136 that originates from the indole moiety and the loss of methylated Asp (*m/z* 162/162). The ions *m/z* 319/325 represent methylated IAAsp after a diagnostic loss of a hexose moiety $[M + H-162]^+$, further described by *m/z* 361/367, which corresponds to a $^{1-5}X_0$-cleaved Glc fragment retained on the IAAsp moiety (Domon and Costello, 1988). From these results we suggest the structure of metabolite 3 to be glucopyranosyl-1-*N*-indole-3-acetyl-*N*-Asp, IAAsp-*N*-glucoside (Fig. 7).

Fast-atom bombardment (FAB) spectra from the methylated and acetylated metabolite 4 gave a double-labeled molecular ion $[M + H]^+/[^{13}C_6M + H]^+$ (*m/z* 520/526). This corresponds to the incorporation of four acetyl groups into a *N*-linked hexose (Fig. 5B). The loss of an acetylated hydroxy group or the loss of the methylated carboxylic acid, $[M-CH_3CO_2]$, is described by *m/z* 460/466. The acetylated Glc is represented by the series of ions with *m/z* 109, 169, and 331. Linked-scan spectra using $[M + H]^+$ (*m/z* 520/526) as parent ions confirmed these fragments were daughter ions. The relative intensities among the acetylated sugar fragments were similar to those of acetylated Glc (*m/z* 169 > *m/z* 271 > *m/z* 211). Mass determination of the $[M]^+/[^{13}C_6M]^+$ of metabolite 4 at a resolution of 5,000 gave *m/z* 519.1767/525.1943 and a calculated elemental composition of $C_{25}H_{29}O_{11}N/^{12}C_{29}{}^{13}C_6H_{29}O_{11}N$ (theoretical value = *m/z* 519.1739/525.1940). The protonated molecular ion of the methylated metabolite 4, *m/z* 352/358 (non-labeled/[$^{13}C_6$]-labeled), and the extracted ion chromatograms also indicated that this metabolite was a glucosylated IAA (Fig. 6B). Verified daughter ions from *m/z* 352/358 were *m/z* 130/136,

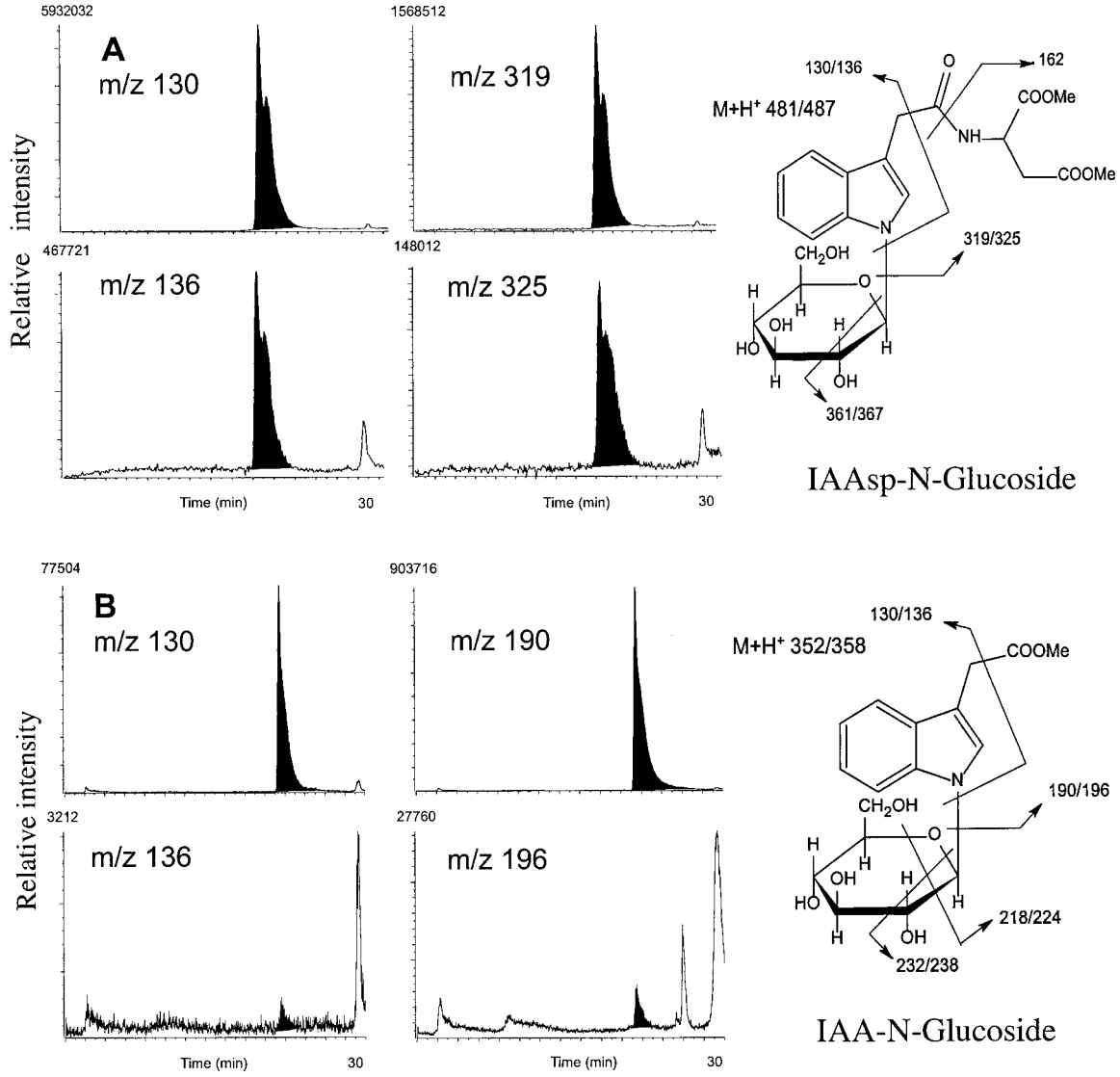


**Figure 6.** The relationship between labeled and unlabeled (endogenous) IAAsp-*N*-glucoside (A) and IAA-*N*-glucoside (B) in Scots pine seedlings presented as ion chromatograms of characteristic ions from the methylated compounds (left) and proposed fragmentation patterns of these compounds (right).

190/196, 218/224, and 232/238. These ions describe the loss of a quinolinium ion (*m/z* 130/136) and the loss of a hexose $[M + H\text{-}162]^+$, leaving methylated IAA (*m/z* 190/196). The ions *m/z* 218/224 and *m/z* 232/238 represent the methylated IAA with a part of the sugar moiety retained after a $^{1-5}X_0$ cleavage and $^{0-2}X_0$ cleavage, respectively. From these results we suggest the structure of metabolite 4 to be glucopyranosyl-1-*N*-indole-3-acetic acid, IAA-*N*-glucoside (Fig. 7).

Spiking experiments with $^{14}C$-labeled compounds indicated that metabolites 5 and 6 were 2-oxindole-3-acetic acid (OxIAA) and IA-Asp, respectively (Figs. 4 and 7), and these conclusions were also verified by HPLC-MS analysis (data not shown). Both these compounds have already been identified as endogenous compounds in Scots pine (Andersson and Sandberg, 1982; Ernstsen et al., 1987).

### Analysis of IAA Metabolism

The relative accumulation of different IAA catabolites was determined by HPLC-radioactive counting (RC) after 24 h of incubating 0- to 10-d-old seeds/seedlings with $^{14}C$-labeled IAA. Rapid induction of IAA metabolism was observed between d 4 and 6 after imbibition (Fig. 8). The primary metabolites were OxIAA and IAAsp (Fig. 7), which started to accumulate on d 4. IAAsp was further metabolized to IAAsp-*N*-glucoside. Minor catabolites were also detected one of which (IAA-*N*-glucoside) appeared si-

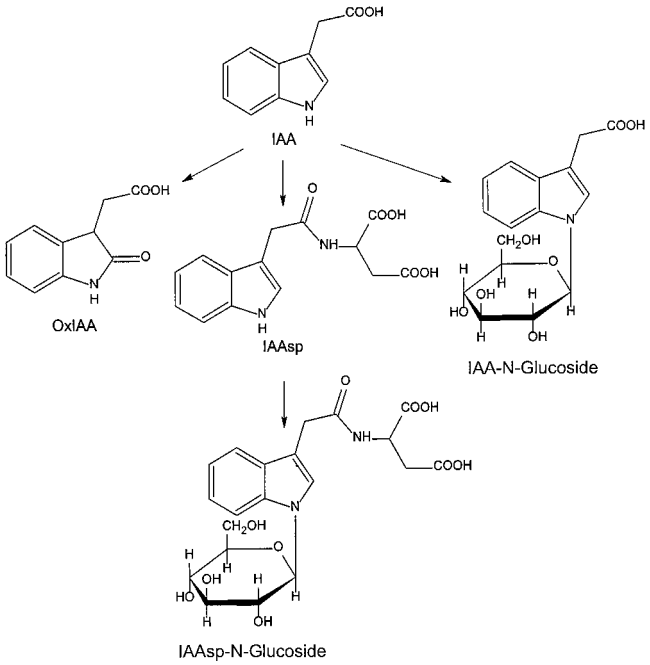


**Figure 7.** Proposed catabolic pathways of IAA in Scots pine seedlings showing the major catabolic products OxIAA and IAAsp, as well as the newly identified IAA conjugates IAAsp-*N*-glucoside and IAA-*N*-glucoside.

multaneously with IAAsp-*N*-glucoside 6 d after imbibition.

## DISCUSSION

### IAA Sources

*Release of Stored Pools*

Indole-3 ethanol (IEt) has previously been shown to be an endogenous constituent of Scots pine needles, probably synthesized from Trp and then further converted to IAA. (Sandberg, 1984). We have also earlier demonstrated that the Scots pine seeds contain IEt conjugates that are released during germination to yield a pulse of free IEt, peaking 2 d after imbibition, and then decreasing rapidly to almost undetectable levels 4 d later (Sandberg et al., 1987). In these previous experiments the content of conjugated IEt and released IEt was of the same size as the IAA pools, indicating that the stored IEt pool is almost certainly a significant contributor to the free IAA pool during the first days of germination. The technique used in the earlier investigation did not involve stable isotopic dilution analysis. $^{14}$C-IAA was used instead to evaluate recovery. This procedure gives a method error of ±20% to 25%, compared with an error of less than ±5% with the techniques used in this investigation. We therefore decided to repeat the analysis of free and bound IAA during germination. The data presented in Figure 1C follow the same general trend we observed earlier (Sandberg et al., 1987). The majority of the IAA in the dry seed is stored as ester-linked conjugates and only a minor part occurs as free IAA or as amide-linked conjugates. The ester-linked pool of IAA is hydrolyzed to yield free IAA, peaking 2 d after imbibition. We have shown (Fig. 2B) that the IAA conjugates are mainly stored in the embryo itself and that only a minor proportion is stored in the general nutrient storage tissue, the megagametophyte. This set of data also demonstrates that the highest concentration of free IAA is localized in the embryo (Fig. 2A). The release of IAA conjugates to yield free IAA in the embryo is a rapid process, which finishes within 4 to 6 d. It thus makes sense for the system to store the conjugated hormone in the embryo itself to allow immediate

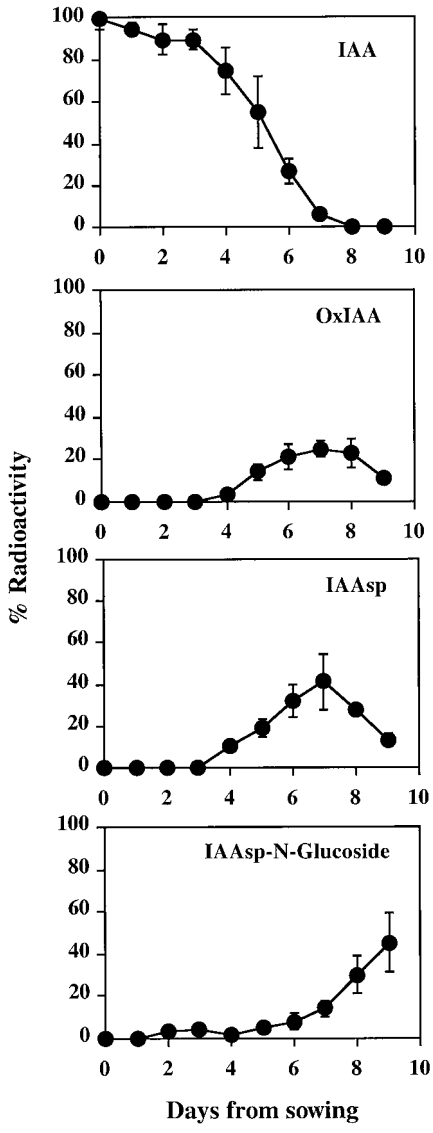


**Figure 8.** Relative IAA catabolism, measured as the amount of radioactivity in each compound after 24 h of incubation with [1-$^{14}$C]IAA. Data presented as the percentage of radioactivity relative to total initially added. Vertical bars represent SD. IAA-*N*-glucoside was present in such low quantities that data for this compound are not presented in this figure.

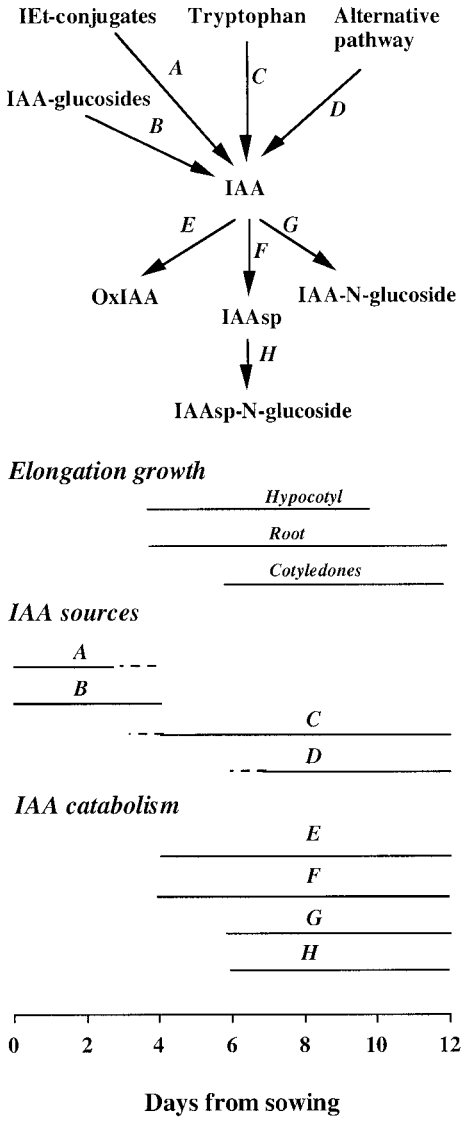


**Figure 9.** A schematic presentation of the timing of metabolic pathways involved in the homeostatic control of the IAA pool size during seed germination and initial seedling growth of Scots pine. The proposed timing of all pathways except A, the release of IEt-conjugates, is based on experimental data from the current study. Pathway A is based on an earlier study (Sandberg et al., 1987).

access and avoid any requirement for long-distance transport. We propose that homeostatic mechanisms like catabolism and conjugation that control IAA levels are not needed in the initial stage of germination, since regulation of the IAA pool size at this stage of development is probably based on adjustment of the hydrolytic activity, releasing free IAA from conjugated pools.

*De Novo Synthesis*

IAA synthesis was assayed in such way that Trp-dependent and Trp-independent IAA synthesis could be distinguished. To simplify the analysis, a relative comparison was performed and no attempt was made to quantify the absolute amount of IAA synthesized. Our data clearly show that both pathways of IAA synthesis were inactive during the initial phase of imbibition and that Trp-dependent synthesis was induced first (Fig. 3A) at around d 4, followed by Trp-independent synthesis around d 7 (Fig. 3B). A clear developmental sequence in utilization of the IAA sources is thus part of the homeostatic regulation in this system. This was also demonstrated by Jensen and Bandurski (1996) who fed deuterated water to dark-grown maize seedlings. Incorporation of deuterium into IAA was not observed in 7-d-old seedlings, although incorporation into Trp could clearly be demonstrated. In Scots pine seedlings ester-linked conjugates are first hydrolyzed to give a peak of free IAA 2 d after imbibition, which coincides with the initial swelling of the seed. This high concentration of free IAA then drops dramatically between d 2 and 5, correlating well with the induction of hypocotyl and root elongation. It is interesting to note that maximum elongation growth is not correlated with the highest level of free IAA. After the stored pools of IAA and IEt have been consumed, Trp-dependent synthesis is induced. For about 2 d, this pathway is then the only active IAA source in the seedling. Around d 6, Trp-independent synthesis is initiated. The differential induction of the two biosynthesis pathways supports the hypothesis that these processes are developmentally controlled. The Trp-dependent synthesis is induced at the same time that the elongation growth of the hypocotyl and root starts, whereas the Trp-independent pathway is induced concurrently with the major elongation phase of the cotyledons. The timing of the induction of Trp-dependent synthesis is consistent with theoretical expectations, since at that point the stored IAA and IEt has been used up and major elongation processes are about to start in the seedling, requiring a direct supply of IAA. This cascade of events is not obviously linked to the Trp-independent synthesis pathway, but it is tempting to speculate that this pathway is localized to the cotyledons, since its induction coincides with the elongation of these organs.

**IAA Catabolism**

The catabolic pathways of IAA in Scots pine have already been demonstrated to involve oxidation of IAA to OxIAA (Ernstsen et al., 1987) and conjugation of IAA to IAAsp (Andersson and Sandberg, 1982). We have identified two new IAA conjugates in this pathway, IAA-*N*-glucoside and IAAsp-*N*-glucoside, sharing a novel *N*-glucoside linkage. Although the FAB-MS fragmentation patterns strongly suggest that the *N*-linked hexose moiety on IAA and IAAsp are Glc, this is not absolutely proven since there are numerous possible IAA conjugates in plants (Doma-

galski et al., 1987). All the carbohydrates previously reported to be conjugated to IAA were linked via the carboxyl group in the side chain (Chisnell, 1984; Domagalski et al., 1987). Feeding experiments with non-labeled/[$^{13}C_6$]-labeled IAA indicate that the endogenous amounts of IAAsp-*N*-glucoside and IAA-*N*-glucoside are very high in germinating Scots pine seedlings, indicating that at least IAA-*N*-glucoside might have a dual function as a catabolite during vegetative growth and possibly as a storage form in the seed. The evidence for this was the high ratio of native to [$^{13}C_6$]-labeled ions in the full scan spectra of IAAsp-*N*-glucoside (Fig. 6A) and in the relative intensity of the daughter ions from the native and [$^{13}C_6$]-labeled IAA-*N*-glucoside molecular ions (Fig. 6B). However, no absolute quantification of the endogenous levels of these new conjugates has yet been done, due to the lack of internal standards.

As shown in Figure 8, there is almost no catabolism of IAA during the first 3 d following imbibition, but thereafter a progressively stronger induction of catabolism occurs, with turnover reaching rapid rates after 6 to 7 d. This fits well with our studies of IAA half-life at d 1, 4, and 7, which also indicate that there is a rapid induction of turnover between d 4 and 7. The two first-labeled catabolites formed are OxIAA and IAAsp, which are synthesized at approximately the same rate starting from d 4. Labeled IAAsp-*N*-glucoside occurs in significant quantities about 2 d after the first appearance of IAAsp and at the same time labeled IAA-*N*-glucoside is observed, but at much lower levels. This also supports our view that the two new conjugates are irreversible inactivation forms of IAA in this system. Precautions have been taken during these experiments to avoid formation of metabolites caused by feeding with unphysiologically high hormone levels, microbiological activity, or the preparation itself (Östin et al., 1998; Catalá et al., 1994). Thus, we are confident that the metabolic profile presented in Figure 4 is representative of the physiological metabolic pathways of IAA in Scots pine seedlings.

### A Developmental Model for IAA Turnover in Scots Pine Seedlings

Figure 9 shows the timing of the different pathways involved in the control of the IAA pool during early seedling growth of Scots pine. A clear difference in function between the two different categories of IAA conjugates is postulated. Ester-linked conjugates of IAA and IEt form a stored pool that is utilized for growth during the initial phase of germination. These conjugates are not involved in a regulatory shunt, i.e. they are not formed at access levels of IAA and, thus after the first 3 d of germination they do not act as sources for release of free IAA. Amide-linked conjugates are only minor constituents in the pool of stored IAA in the seed. The formation of OxIAA and IAAsp is induced around 4 d after germination, together with the other minor catabolites, and IAAsp, as well as the new *N*-linked sugar conjugates are believed to serve less as a storage form of IAA than as intermediates in irreversible catabolism. There is no catabolism of IAA during the initial growth phase when the predominant IAA sources are IAA and IEt conjugates, but as soon as de novo synthesis begins, catabolism is induced. The close correlation between the induction of de novo synthesis and catabolism indicates that the homeostatic system is dependent on mechanisms such as catabolism and conjugation to control the IAA pool size.

## MATERIALS AND METHODS

### Chemicals and Isotopically Labeled Substrates

[1′-$^{14}$C]IAA with a specific activity of 55 mCi/mmol was purchased from American Radiolabeled Chemicals (St. Louis). [$^{13}C_6$]IAA and [$^{15}N_1$]Trp were from Cambridge Isotope Laboratories (Andover, MA). [$^2H_5$]IAA was supplied by MSD Isotopes (Montreal). Deuterated water came from Norsk Hydro (Porsgrunn, Norway). Labeled IAAsp, and OxIAA were synthesized from [1′-$^{14}$C]IAA according to the methods of Tuominen et al. (1994) and Ilic et al. (1997). The Murashige-Skoog medium was from Duchefa (Harlem, The Netherlands), and all other chemicals were from Sigma (St. Louis) if not stated otherwise.

### Plant Material and Growth Conditions

The Scots pine (*Pinus sylvestris*) seeds used were from a local seed orchard (Östteg, Umeå, Sweden; 63°55′N, 19°45′E) and had a germination rate of 95.7%. For anatomical and metabolic studies, fully developed seeds were selected and germinated in Petri dishes on moist filter paper at 20°C under 155 $\mu$mol photons $m^{-2}$ $s^{-1}$ of constant light. Germination counts were taken every day for 10 d among five replicate sets, each of 100 seeds. Seeds with visible roots were counted as germinated. After removal of the seed coat, seeds were fixed in 2.5% (v/v) glutaraldehyde for at least 24 h before embedding in Technovit 7100 (Heraeus Kulzer, Wehrheim, Germany). The embedded specimens were sectioned in a microtome (Microm HM 350 Rotary, Walldorf, Germany) and stained with toluidine blue. Pictures were obtained using a microscope (Axioplan, Zeiss, Jena, Germany) equipped with a camera (MC80, Zeiss). For the identification of IAA metabolites, seeds were surface sterilized by incubation in 1% (w/v) calcium hypochlorite plus 0.02% (v/v) Triton X-100 for 20 min, rinsed in sterile water, and incubated overnight at 4°C. The seeds were then germinated for 10 d in darkness on moist filter papers at room temperature. To obtain enough material for the initial identification studies, expanding shoots from 4-year-old plants grown in a greenhouse were also used.

### Quantification of IAA and IAA Conjugates

For analysis of endogenous IAA levels, 100 mg of seeds were harvested 0 to 10 d after imbibition and were homogenized in liquid nitrogen. Subsamples of 10 mg were extracted, purified, and analyzed by GC-selected reaction monitoring-MS as described in Edlund et al. (1995). Calculation of isotopic dilution was based on the addition of 50 pg [$^{13}C_6$]IAA/1 mg tissue. After mild and strong alkaline hydrolysis, respectively, procedures outlined by Sundberg (1990) were used to analyze IAA-ester and IAA-amide conjugates. Pooled material (0.5–1 mg) was used for analysis of IAA levels in embryos and the megagametophytes. Calculation of isotopic dilution was in this case based on the addition of 25 pg [$^{13}C_6$]IAA per sample. Samples were prepared in an ultra-clean environment and random blank samples were analyzed to detect possible contamination problems associated with the analysis of extremely low amounts of IAA. Measurements are presented as the means from five to six individual samples.

### IAA Biosynthesis from [$^{15}N_1$]Trp and Deuterated Water

Four hundred milligrams of seeds were incubated for 6 h with 2 $\mu$g of [$^{15}N_1$]Trp 1, 4, and 7 d after imbibition. The seeds were rinsed in distilled water and left on moist filter paper in darkness for the remainder of the experiment. Approximately 10-mg samples were collected at 6, 12, 24, 36, and 48 h. Four hundred milligrams of seeds were also incubated with deuterated water for 48-h periods starting at d 1, 4, and 7 after imbibition. Samples were collected as described above. The tissue was extracted after the addition of 50 pg [$^{13}C_6$]IAA/1 mg tissue as an internal standard and, after purification, [$^{15}N_1$]IAA, deuterium-labeled IAA, and endogenous IAA were analyzed by GC-MS (operated in the selected ion monitoring mode, R = 5000). No attempts were made to calculate exact synthesis rates. Incorporation of $^{15}N_1$ from Trp into IAA is expressed as the ratio of the labeled to unlabeled IAA base peaks (*m/z* 203.102 and 202.105, respectively). Incorporation of $^2H$ from deuterated water into IAA is expressed as the ratio of deuterium-labeled IAA (*m/z* 203.111 + 204.118) to unlabeled IAA (*m/z* 202.105).

### Turnover of [$^{13}C_6$]IAA

Four hundred milligrams of seeds was incubated for 5 h with 100 ng of [$^{13}C_6$]IAA dissolved in 5% (v/v) ethanol, 1, 4, and 7 d after imbibition. The seeds were rinsed in distilled water and left on moist filter paper in darkness for the remainder of the experiment. Approximately 10-mg samples were collected at 0, 3, 6, 9, 12, and 24 h for the incubations starting at d 4 and 7, and at 6, 12, 24, and 48 h for the incubation starting at d 1. Free IAA was extracted and purified as described above, except for the addition of 100 ng [$^2H_5$]IAA as an internal standard for the quantification of IAA. GC-MS (operated in the selected ion monitoring mode, R = 5000) was performed using *m/z* 207.137 and 266.149 for measuring [$^2H_5$]IAA, *m/z* 208.125 and 267.139 for [$^{13}C_6$]IAA, and *m/z* 202.105 and 261.118 for endogenous IAA. The obtained values were corrected for "crosstalk" between the *m/z* 208.125/207.137 and *m/z* 267.139/266.149 channels.

### Identification of IAA Metabolites

To produce large amounts of metabolites, pine shoots were placed in vials with 0.5 mL of incubation media containing a mixture of 100 $\mu$M [$^{13}C_6$]IAA, 100 $\mu$M IAA, and 10 $\mu$M [1′-$^{14}$C]IAA in one-half-strength Murashige and Skoog medium. The medium with tracers was taken up via the transpiration stream and excess one-half-strength Murashige and Skoog medium was thereafter added to provide the plant with enough liquid for the rest of the incubation period. Samples were collected for analysis after 24 h. To verify the existence of the metabolites in the plant system under study, sterile seedlings with removed roots were immersed in the same incubation media containing tracers for 24 h. Shoots and seedlings were frozen in liquid nitrogen, homogenized, and extracted with methanol containing 0.2% (w/v) antioxidant (diethyldithiocarbamic acid) for 4 h. After filtration, 10 mL of 50 mM sodium phosphate buffer, pH 7, was added and the sample was reduced to water phase in a rotary evaporator. Seedling extracts could then be taken directly to the solid phase extraction step (see below), whereas shoot extracts first had to be subjected to solvent partitioning against ethyl acetate and water-saturated butanol (Östin et al., 1998). Solid-phase extraction was carried out to purify each sample prior to HPLC. The dried sample was dissolved in 1% (v/v) acetic acid (HAc) and passed through a 1-g C18 SPE-column (Varian, Harbor City, CA). The column was rinsed with 10 mL of 1% (v/v) HAc and eluted with 2 × 5 mL of 80% (v/v) methanol and then with 5 mL of methanol. All fractions containing radioactivity were kept and dried. The samples were dissolved in 10 $\mu$L of methanol, diluted with 1% (v/v) HAc, and centrifuged at 14,000 rpm for 5 min. The supernatant was then fractionated by HPLC-RC (Östin et al., 1998). Aliquots of labeled fractions from the HPLC-RC were subjected to mild or strong alkaline hydrolysis (Sundberg, 1990) and any released IAA was extracted with ethyl acetate and reanalyzed on HPLC-RC. To isolated metabolites, $^{14}$C-labeled standards were added to verify their identity by HPLC-RC. To improve sensitivity and chromatography in HPLC-MS, the isolated metabolites were methylated with ethereal diazomethane according to Shlenk and Gellerman (1960). A second round of purification could then be done using the same HPLC-system, prior to further HPLC-MS analysis. Metabolites believed to contain a sugar moiety were acetylated (Connors and Pandit, 1978) with *N*-methyl imidazole and acetic anhydride. The capillary HPLC-frit-FAB-MS system used for the identification of IAA metabolites has already been described in detail (Östin 1995). B/E-linked scanning of selected metastable ions in the first field free region was used to determine daughter ion spectra and to provide selected reaction monitoring. Accurate mass determination was done by electrostatic field scanning at a resolution of 5,000. Polyethylene glycol 300 and 600 (0.2% [v/v]of each) were

added to the mobile phase as internal reference compounds. Daughter ion spectra from *m/z* 331 of acetylated Gal, Glc, Fru, lactose, and Man standards were obtained for comparison with the daughter ion spectra of the sugar moieties obtained from the protonated molecular ions of the acetylated metabolites.

### Analysis of IAA Metabolism

Seeds (500 mg) were incubated in 5 $\mu$M [1-$^{14}$C]IAA in one-half-strength Murashige and Skoog medium, pH 5.6, in the dark for 24 h 0 to 10 d after imbibition. The plant material was homogenized in liquid nitrogen, extracted, purified, and analyzed by HPLC-RC (Östin et al., 1998). The relative abundance of different IAA metabolites is presented as the percentage of radioactivity in each compound relative to the total amount of radioactivity initially added to the sample.

## ACKNOWLEDGMENTS

The authors are grateful to Gun Lövdahl and Kjell Olofsson for skillful technical assistance.

Received May 1, 2000; modified July 18, 2000; accepted September 18, 2000.

## LITERATURE CITED

**Andersson B, Sandberg G** (1982) Identification of endogenous *N*-(3-indoleacetyl) aspartic acid in Scots pine (*Pinus sylvestris* L.) by combined gas chromatography-mass spectrometry, using high-performance liquid chromatography for quantification. J Chromatogr **238:** 151–156

**Bandurski RS, Cohen JD, Slovin JP, Reinecke DM** (1995) Auxin biosynthesis and metabolism. *In* PJ Davies, ed, Plant Hormones. Kluwer Academic Publishers, Dordrecht, The Netherlands, pp 39–65

**Bartel B** (1997) Auxin biosynthesis. Annu Rev Plant Physiol **48:** 51–67

**Catalá C, Crozier A, Chamarro J** (1994) Decarboxylative metabolism of [1′-14C]-indole-3-acetic acid by tomato pericarp discs during ripening. Planta **193:** 508–513

**Chisnell JR** (1984) Myo-inositol esters of indole-3-acetic acid are endogenous components of *Zea mays* L. shoot tissue. Plant Physiol **74:** 278–283

**Connors KA, Pandit NK** (1978) *N*-methylimidazole as a catalyst for analytical acetylations of hydroxy compounds. Anal Chem **50:** 1542–1545

**Domagalski W, Schulze A, Bandurski RS** (1987) Isolation and characterization of esters of indole-3-acetic acid from the liquid endosperm of horse chestnut (*Aesculus* species) Plant Physiol **84:** 1107–1113

**Domon B, Costello CE** (1988) A systematic nomenclature for carbohydrate fragmentations in FAB-MS/MS spectra of glucoconjugates. Glycoconjugate J **5:** 397–409

**Edlund A, Eklöf S, Sundberg B, Moritz T, Sandberg G** (1995) A microscale technique for gas-chromatography mass-spectrometry measurements of picogram amounts of indole-3-acetic acid in plant-tissues. Plant Physiol **108:** 1043–1047

**Epstein E, Cohen JD, Bandurski RS** (1980) Concentration and metabolic turnover of indoles in germinating kernels of *Zea mays* L. Plant Physiol **65:** 415–421

**Ernstsen A, Sandberg G** (1986) Identification of 4-chloroindole-3-acetic acid and indole-3-aldehyde in seeds of *Pinus sylvestris*. Physiol Plant **68:** 511–518

**Ernstsen A, Sandberg G, Lundström K** (1987) Identification of oxindole-3-acetic acid, and metabolic conversion of indole-3-acetic acid to oxindole-3-acetic acid in seeds of *Pinus sylvestris*. Planta **172:** 47–52

**Estelle M** (1998) Polar auxin transport: new support for an old model. Plant Cell **10:** 1775–1778

**Ilic N, Magnus V, Östin A, Sandberg G** (1997) Stable-isotope labeled metabolites of the phytohormone, indole-3-acetic acid. J Label Compd Radiopharm **39:** 433–440

**Jensen PJ, Bandurski RS** (1996) Incorporation of deuterium into indole-3-acetic acid and tryptophan in *Zea mays* seedlings grown on 30% deuterium oxide. J Plant Physiol **147:** 697–702

**Michalczuk L, Ribnicky DM, Cooke T, Cohen JD** (1992) Regulation of indole-3-acetic acid pathways in carrot cell cultures. Plant Physiol **100:** 1346–1353

**Miller AN, Walsh CS, Cohen JD** (1987) Measurement of indole-3-acetic acid in peach fruit (*Prunus persica* L. Batsch cv Redhaven) during development. Plant Physiol **84:** 491–494

**Normanly J** (1997) Auxin metabolism. Physiol Plant **100:** 431–442

**Normanly J, Bartel B** (1999) Redundancy as a way of life: IAA metabolism. Curr Opin Plant Biol **2:** 207–213

**Normanly J, Cohen JD, Fink GR** (1993) *Arabidopsis thaliana* auxotrophs reveal a tryptophan-independent biosynthetic pathway for indole-3-acetic acid. Proc Natl Acad Sci USA **90:** 10355–10359

**Normanly J, Slovin JP, Cohen JD** (1995) Rethinking auxin biosynthesis and metabolism. Plant Physiol **107:** 323–329

**Östin A** (1995) Metabolism of indole-3-acetic acid in plants with emphasis on non-decarboxylative catabolism. PhD thesis. The Swedish University of Agricultural Sciences, Umeå

**Östin A, Kowalczyk M, Bhalerao RP, Sandberg G** (1998) Metabolism of indole-3-acetic acid in *Arabidopsis*. Plant Physiol **118:** 285–296

**Östin A, Moritz T, Sandberg G** (1992) Liquid chromatography-mass spectrometry of conjugates and oxidative metabolites of indole-3-acetic acid. Biol Mass Spectrom **21:** 292–298

**Ribnicky DM, Nebojsa I, Cohen JD, Cooke TJ** (1996) The effects of exogenous auxins on endogenous indole-3-acetic acid metabolism: the implications for carrot somatic embryogenesis. Plant Physiol **112:** 549–558

**Sandberg G** (1984) Biosynthesis and metabolism of indole-3-ethanol and indole-3-acetic acid by *Pinus sylvestris* needles. Planta **161:** 398–403

**Sandberg G, Ernstsen A** (1987) Dynamics of indole-3-acetic acid during germination of *Picea abies* seeds. Tree Physiol **3:** 185–192

**Sandberg G, Ernstsen A, Hamnede M** (1987) Dynamics of indole-3-acetic acid and indole-3-ethanol during development and germination of *Pinus sylvestris* seeds. Physiol Plant **71:** 411–418

**Shlenk H, Gellerman JL** (1960) Esterification of fatty acids with diazomethane on a small scale. Anal Chem **32:** 1412–1414

**Sitbon F, Åstot C, Eklund A, Crozier A, Sandberg G** (2000) The relative importance of tryptophan-dependent and tryptophan-independent biosynthesis of indole-3-acetic acid in tobacco during vegetative growth. Planta **211:** 715–721

**Sundberg B** (1990) Influence of the extraction solvent (buffer, methanol, acetone) and time on the quantification of indole-3-acetic acid in plants. Physiol Plant **78:** 293–297

**Tam YY, Slovin JP, Cohen JD** (1995) Selection and characterization of $\alpha$-methyltryptophan-resistant lines of *Lemna gibba* showing a rapid rate of indole-3-acetic acid turnover. Plant Physiol **107:** 77–85

**Tuominen H, Östin A, Sandberg G and Sundberg B** (1994) A novel metabolic pathway for indole-3-acetic acid in apical shoots of *Populus tremula* (L.) × *Populus tremuloides* (Michx.). Plant Physiol **106:** 1511–1520